HAIT Journal of Science and Engineering B, Volume 2, Issues 5-6, pp. 715-735

A modified DTC-SVM for sensorless matrix converter drives using a simple deadbeat scheme

Kyo-Beum Lee* and Frede Blaabjerg

Institute of Energy Technology, Aalborg University
Pontoppidanstraede 101, DK-9220 Aalborg East, Denmark
**Corresponding author: kyl@iet.aau.dk*

Received 1 March 2005, accepted 10 June 2005

Abstract

In this paper, a modified direct torque control (DTC) for matrix converter drives is proposed which enables to minimize torque ripple and to obtain unity input power factor, while maintaining constant switching frequency. It is possible to combine the advantages of matrix converters with the advantages of the DTC strategy using the basic DTC scheme. However, some drawbacks, such as large torque ripple in the low speed region and switching frequency variation according to the change of the motor speed and the amplitude of hysteresis bands, still exist. In the proposed scheme, a modified DTC strategy for matrix converter drives is derived using space vector modulation and flux deadbeat algorithm. Experimental results are shown to illustrate the feasibility of the proposed strategy.

1 Introduction

The induction motor drive fed by a matrix converter is superior to the conventional inverter because of the lack of bulky DC-link capacitors with limited life time, the bi-directional power flow capability, the sinusoidal input/output currents, and adjustable input power factor. Furthermore, because of a high integration capability and higher reliability of the semiconductor structures, the matrix converter topology is recommended for extreme temperatures and critical volume/weight applications. However, only

a few of the practical matrix converters have been applied to induction motor drive system because the implementation of switch devices in the matrix converter is difficult and modulation technique and commutation control are more complicated than in the conventional PWM inverter [1–3].

The Direct Torque Control (DTC) scheme for matrix converter drives was initially presented in [4]. The generation of the voltage vectors required to implement the DTC of induction motors under the constraint of unity input power factor was allowed. However, the DTC scheme using a switching table has some drawbacks. Switching frequency varies according to the motor speed and the hysteresis bands of torque and flux, large torque ripple is generated in a low speed range because of small back EMF of the induction motor, and a high control sampling frequency is required to achieve good performance [5]. Although several methods to solve these problems have been presented [6–11], these methods are designed for a conventional inverter drive system. On the contrary, research results to solve these problems for matrix converter drives have not been reported in the literature.

In this paper, a new DTC scheme using SVM and a deadbeat algorithm for matrix converter drives is presented, which enables to minimize torque ripple and obtain unity input power factor, while maintaining constant switching frequency. To improve the low-speed operation performance, an adaptive observer is employed for the estimation of the stator flux, the rotor speed, and the stator resistance [12]. In addition, a matrix converter model for low speed operation is used to realize high performance control [3]. The proposed whole control scheme of sensorless DTC for induction motor drives fed using a matrix converter is shown in Fig. 3, which consists of a simple deadbeat controller, input voltage angle calculator, indirect space vector modulation, an adaptive observer for speed and rotor flux estimation, and nonlinear modeling of matrix converter. Experimental results are presented to verify the effectiveness and feasibility of the proposed control system.

2 Indirect space vector modulation of matrix converter drives

The most general modulation method for matrix converter is the Indirect Space Vector Modulation (ISVM), which considers the matrix converter as a two stage transformation converter: a rectification stage to provide a constant imaginary DC-link voltage per switching period and an inverter stage to produce the three output voltages.

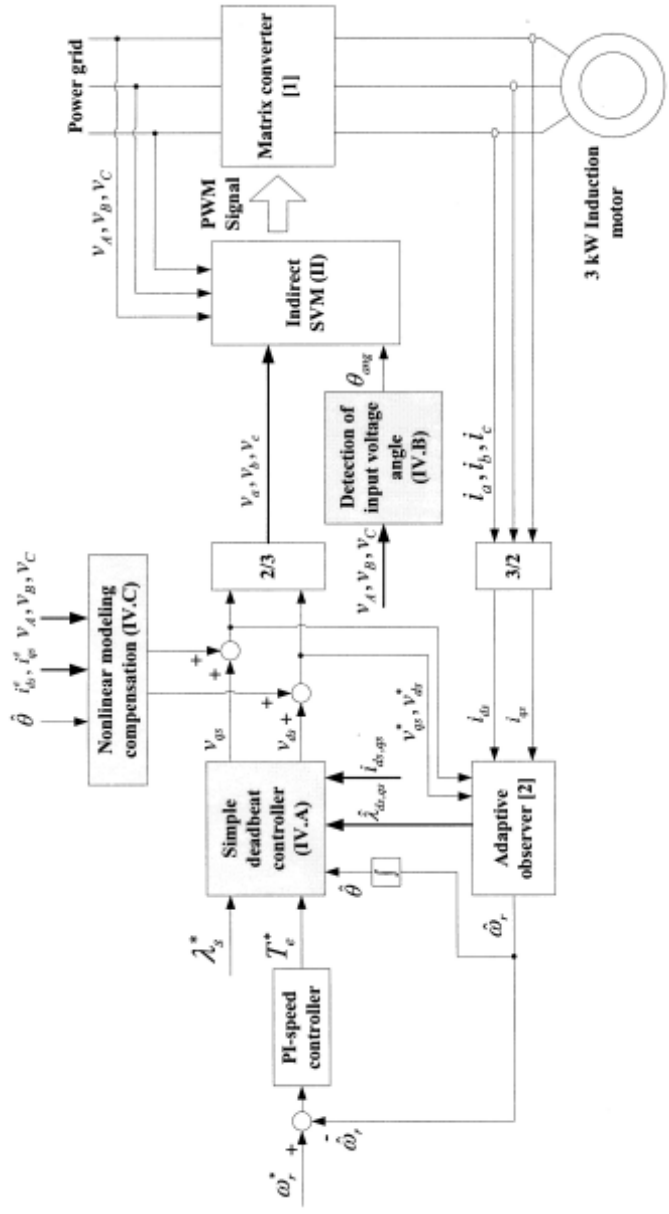

Figure 1: The proposed sensorless DTC for matrix converter drives.

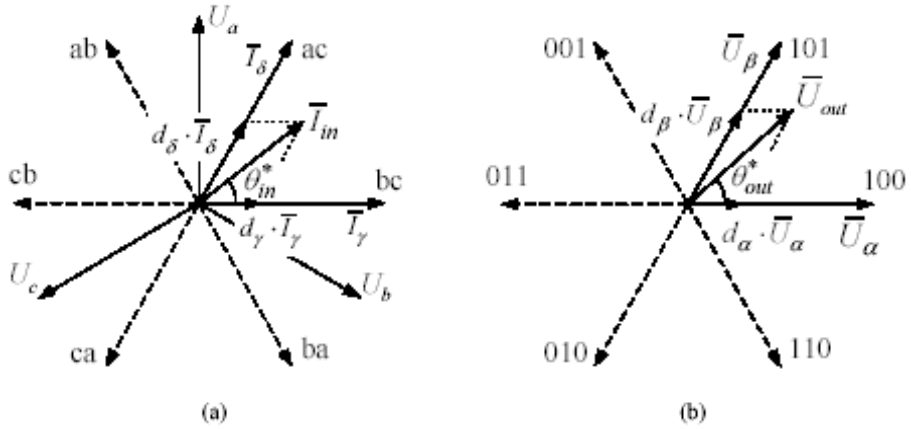

Figure 2: Generation of the reference voltage vectors using ISVM (a) in the rectification stage, (b) in the inversion stage.

The input current vector, I_{in}, that corresponds to the rectification stage and the output voltage vector, U_{out}, that corresponds to the inversion stage are the reference vectors (Fig. 2). The indirect space vector modulation uses a combination of the two adjacent vectors and a zero vector to produce the reference vector. The ratio between the two adjacent vectors duty cycle determines the magnitude of the reference vector. The duty cycles of the active switching vectors for the rectification stage, I_γ, I_δ, are calculated with (1) and the duty cycle of the active switching vectors for the inversion stage, U_α, U_β are calculated with (2).

$$d_\gamma = m_I \sin\left(\frac{\pi}{3} - \theta^*_{in}\right) \text{ and } d_\delta = m_I \sin\theta^*_{in} \tag{1}$$

$$d_\alpha = m_U \sin\left(\frac{\pi}{3} - \theta^*_{out}\right) \text{ and } d_\beta = m_U \sin\theta^*_{out} \tag{2}$$

where m_I and m_U are the rectification and inversion stage modulation indexes, θ^*_{in} and θ^*_{out} are the angles within their respective sectors of the input current and output voltage reference vectors (see Fig. 2).

To obtain a correct balance of the input currents and the output voltages in the same switching period, the modulation pattern should produce all combinations of the rectification $(\gamma - \delta - 0)$ and the inversion $(\alpha - \beta - 0)$ switching states, resulting in the following switching pattern: $\alpha\gamma - \alpha\delta - \beta\delta - \beta\gamma - 0$. Therefore, each sequence duty cycle is a result of cross products of

the rectification and the inversion stage duty cycles, while the duration of the zero-vector is completing the switching sequence as

$$\begin{aligned} &d_{\alpha\gamma} = d_\alpha d_\gamma, \quad d_{\alpha\delta} = d_\alpha d_\delta, \quad d_{\beta\delta} = d_\beta d_\delta, \quad d_{\beta\gamma} = d_\beta d_\gamma, \\ &d_0 = 1 - (d_{\alpha\gamma} + d_{\alpha\delta} + d_{\beta\delta} + d_{\beta\gamma})\,. \end{aligned} \tag{3}$$

The duration of each sequence is found by multiplying the corresponding duty cycle by the switching period.

3 DTC for matrix converter drives

The principle of the DTC is briefly discussed and a torque, flux, and power factor control for matrix converter system is studied in this section. The DTC is a hysteresis torque and stator flux control that directly selects one of the six nonzero and two zero voltage vectors generated by a conventional two-level inverter in order to maintain the estimated stator flux and torque within the hysteresis bands. Fig. 3 shows a space vector representation of the conventional inverter output voltages.

From the induction motor equations with the voltage drop across the stator resistance neglected, the relationship between the inverter output voltage vector and the variation of the stator flux can be expressed as

$$\Delta\bar{\lambda}_s = (\bar{v}_s - \bar{\imath}_s R_s)\, t_{sp} = \bar{e}_s t_{sp} \approx \bar{v}_s t_{sp} \tag{4}$$

where $\bar{v}_s$ is the inverter output voltage vector, R_s is the stator resistance, $\bar{e}_s$ is the electromotive force, and t_{sp} is the sampling period.

Equation (4) shows that an applied stator voltage vector produces a stator flux change. The amplitude of the stator flux change is proportional to the product of the applied voltage vector and the sampling period. The vectorial direction of the stator flux change coincides with that of the selected voltage vector.

The relationship between the stator and rotor fluxes is

$$\bar{\lambda}_r = \frac{L_m}{L_s} \frac{1}{1 + s\sigma\tau_r} \bar{\lambda}_s \tag{5}$$

where R_r is the rotor resistance, L_s, L_r are the stator and rotor self inductances, L_m is the mutual inductance, $\tau_r = L_r/R_r$ is the rotor time constant, $\sigma = 1 - L_m^2/L_s L_r$ is the leakage coefficient, $\bar{\lambda}_s$ is the stator flux vector, and $\bar{\lambda}_r$ is the rotor flux vector.

The electromagnetic torque in the induction motor can be expressed as

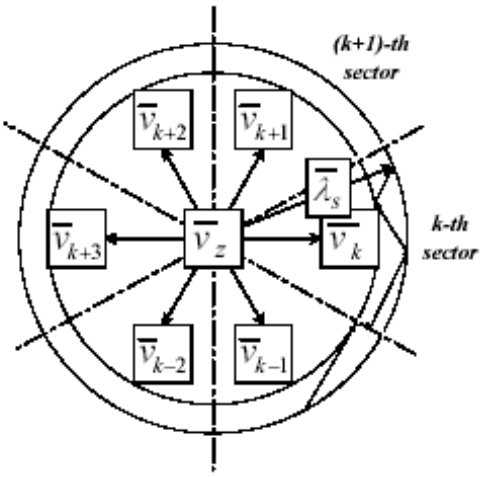

Figure 3: The output voltage vectors in a conventional inverter system.

$$T_e = \frac{3}{2}P\frac{L_m}{\sigma L_s L_r}\bar{\lambda}_s \cdot j\bar{\lambda}_r = \frac{3}{2}P\frac{L_m}{\sigma L_s L_r}\lambda_s\lambda_r \sin\theta_{sr} \tag{6}$$

where θ_{sr} is the angle between the stator and rotor flux vectors, and P is the number of pole-pairs.

Equation (6) shows that torque is determined by the magnitudes and the phase angle of the stator and rotor fluxes. The switching look-up table is shown in Table 1.

$\bar{\lambda}_s$ in sector k		Torque	
		$\uparrow$	$\downarrow$
Flux	$\uparrow$	$\bar{v}_{k+1}$	$\bar{v}_z$
	$\downarrow$	$\bar{v}_{k+2}$	$\bar{v}_z$

Table 1. Switching look-up table.

Normally, the matrix converter is fed by a voltage source and, for this reason, the input terminal should not be directly short circuit. On the other hand, the load has typically an inductive nature and, for this reason, an output phase must never be opened.

Defining the switching function of a single switch as

$$S_{Kj} = \begin{cases} 1, \text{ switch } S_{Kj} \text{ closed} \\ 0, \text{ switch } S_{Kj} \text{ open} \end{cases} \tag{7}$$

where $K = \{A,\ B,\ C\}$ is the input phase and $j = \{a,\ b,\ c\}$ is the output phase.

The constraints discussed above can be expressed by

$$S_{Aj} + S_{Bj} + S_{Cj} = 1. \tag{8}$$

With these restrictions, the 3×3 matrix converter has 27 possible switching states.

Let $m_{Kj}(t)$ be the duty cycle of switch S_{Kj}, defined as

$$m_{Kj}(t) = t_{Kj}/t_{sp} \text{ where } 0 < m_{Kj} < 1. \tag{9}$$

The low-frequency transfer matrix converter is defined by

$$\mathbf{M}(t) = \begin{bmatrix} m_{Aa}(t) & m_{Ba}(t) & m_{Ca}(t) \\ m_{Ab}(t) & m_{Bb}(t) & m_{Cb}(t) \\ m_{Ac}(t) & m_{Bc}(t) & m_{Cc}(t) \end{bmatrix}. \tag{10}$$

The low-frequency component of the output phase voltage v_o is given by

$$\bar{v}_o(t) = \mathbf{M}(t) \cdot \bar{v}_i(t) \tag{11}$$

where $\bar{v}_o$ is the output voltage vector and $\bar{v}_i$ is the input voltage vector.

The low-frequency component of the input current i_i is

$$\bar{i}_i(t) = \mathbf{M}(t)^T \cdot \bar{i}_o(t) \tag{12}$$

where $\bar{i}_i$ is the input current vector and $\bar{i}_o$ is the output current vector.

It appears that the matrix converter generates a higher number of output voltage vectors with respect to a conventional two-level inverter. In the DTC for matrix converter drives, the average value of the sine of the displacement angle θ_{dis} between the input line-to-neutral voltage vector and the corresponding input line current vector has been chosen as a third variable. The DTC for matrix converter drives selects the proper switching configuration at each sampling time, which allows the compensation of instantaneous errors in the flux magnitude and torque, under the constraint of unity input power factor. The last requirement of the input side of the matrix converter is intrinsically satisfied if the average value of sin (θ_{dis}) is maintained close to zero. The average value of sin (θ_{dis}) is obtained by applying a low-pass filter to its instantaneous values. A schematic diagram of the DTC for a matrix converter drive is represented in Fig. 4.

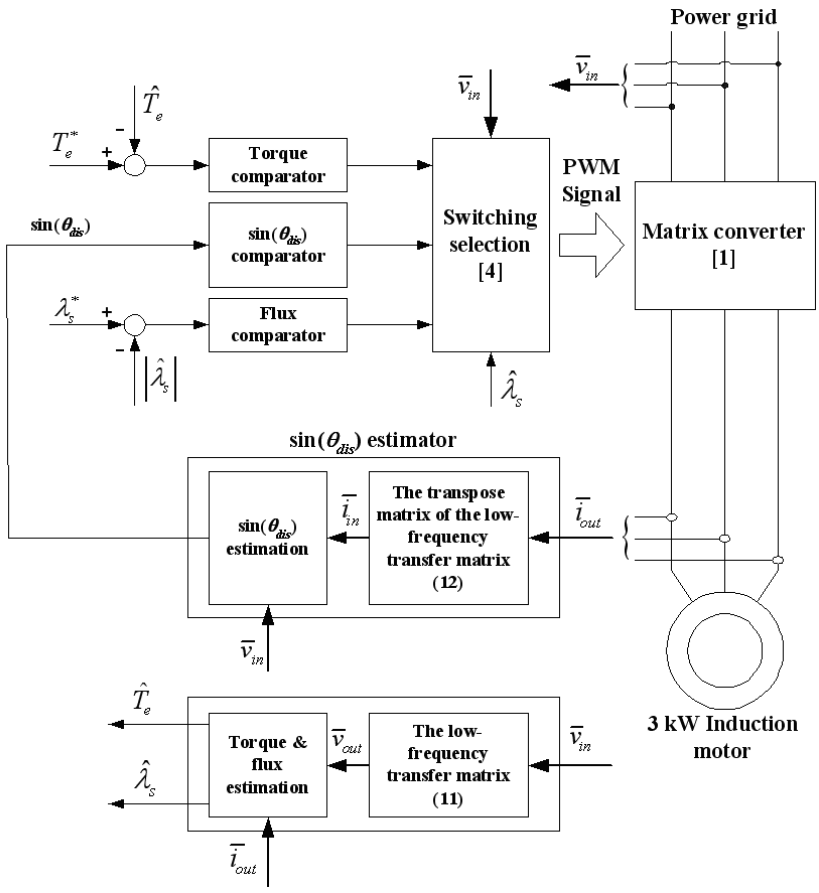

Figure 4: The DTC for matrix converter drives.

The reference value of the torque and the stator flux magnitude are compared with the estimated value. The output of the hysteresis comparators, the stator flux, and input line-to-neutral voltage vector are the input to the switching selection algorithm [4]. The displacement estimator requires the knowledge of input voltages and output currents. However, only the input voltages and output currents are measured, while the other quantities are calculated on the basis of the low-frequency transfer matrix shown in Fig. 4.

4 A modified DTC using SVM and a deadbeat control

The previously mentioned basic DTC for matrix converter drives allows for the generation of the voltage vectors required to implement the DTC of the induction motor under the constraint of unity input power factor. However, the switching frequency varies according to the motor speed and the hysteresis bands of torque and flux, large torque ripple is generated in a low speed range because of small back EMF of an induction motor, and high control sampling time is required to achieve good performance. To cope with these problems, a new modified DTC is proposed. The proposed scheme is shown in Fig. 5 and Fig. 6, which consists of a deadbeat controller and input voltage angle calculation.

4.1 A modified DTC using SVM and simple deadbeat scheme

The proposed sensorless DTC for matrix converter drives is presented in Fig. 1, and the internal structure of the deadbeat controller is shown in Fig. 5.

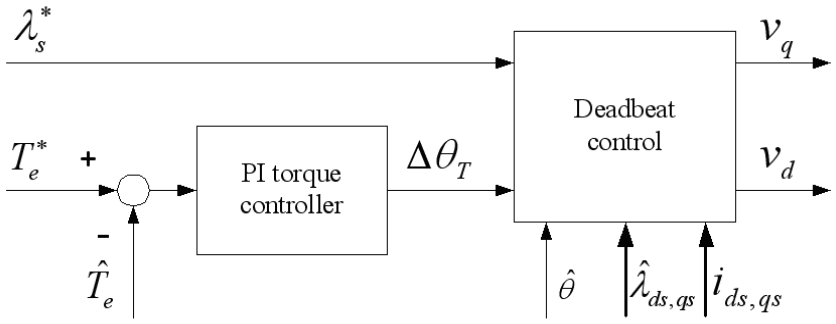

Figure 5: The block diagram of the simple deadbeat controller.

In the proposed control system, a PI-torque controller and a deadbeat control scheme are used to determine the reference voltage vector for space vector modulation instead of torque and flux hysteresis controller for the switching vector table. The reference torque and the reference stator flux amplitude are delivered to the flux deadbeat controller. When the estimated torque is below the reference torque, the PI-torque controller generates the

load angle increment to force the stator flux to rotate at higher speed, such that the instantaneous error between reference torque and estimated torque is reduced to zero (see Eq. 6). The stator voltage equation of induction motors in the stationary reference frame is shown in (13). The reference values of d- and q- axis stator voltage are calculated taking into account the stator resistance, PI-torque controller output, estimated stator flux magnitude, actual stator currents, and rotor position.

$$\bar{v}_s = \frac{d\bar{\lambda}_s}{dt} + R_s \bar{i}_s. \tag{13}$$

Ideally, a deadbeat controller would establish zero flux error within one sampling period t_{sp}. It is necessary to impose the stator voltage at the $(k+1)^{th}$ sampling time, resulting in

$$\bar{\lambda}_{s,\,k+1} = \bar{\lambda}^*_{s,\,k}. \tag{14}$$

Equation (13) can be written in a discrete form by substituting (14) into (13):

$$\begin{aligned} \bar{v}_{s,\,k+1} = \frac{\bar{\lambda}^*_{s,\,k} - \bar{\lambda}_{s,\,k}}{t_{sp}} + R_s \bar{i}_{s,\,k+1} = \frac{\left|\bar{\lambda}^*_{s,\,k}\right| \cos\left(\hat{\theta} + \Delta\theta_T\right) - \left|\bar{\lambda}_{s,\,k}\right| \cos\left(\hat{\theta}\right)}{t_{sp}} + R_s \bar{i}_{s,\,k+1} \\ + j \left(\frac{\left|\bar{\lambda}^*_{s,\,k}\right| \sin\left(\hat{\theta} + \Delta\theta_T\right) - \left|\bar{\lambda}_{s,\,k}\right| \sin\left(\hat{\theta}\right)}{t_{sp}} + R_s \bar{i}_{s,\,k+1} \right), \end{aligned} \tag{15}$$

where $\bar{i}_{s,\,k+1} = (2-\alpha)\,\bar{i}_{s,\,k} - (1+\alpha)\,\bar{i}_{s,\,k-1}$ and α is a positive constant, $0 \leq \alpha < 1$.

In this simple deadbeat and current predictive scheme, the reference voltage at the $(k+1)^{th}$ sampling time is calculated by using the system values at the k^{th} and $(k-1)^{th}$ sampling time. In (15), the reference voltage value at $(k+1)^{th}$ sampling time for space vector modulation is calculated by using the stator flux, the load angle, and actual current at the k^{th} sampling time and its sampling before.

When the magnitude of the reference voltage vector $\mathbf{v}^*$ significantly exceeds the maximum realizable value, the inverter control of switched to the basic DTC block shown in Fig. 4. In this way, the drive combines advantages of the smooth steady-state operation and rapid response to control commands.

4.2 Detection of input voltage angle

To implement the ISVM (Indirect Space Vector Modulation), the input reference current vector is given by the input voltage vector for an instantaneous unity power factor. Under balanced conditions, the angular velocity as well as the magnitude of the input voltage vector is constant. In this situation the determination of the input current reference angle is quite straightforward. Unfortunately, with unbalanced supply voltages, the negative sequence component of the voltage causes variation in magnitude and angular velocity of the input voltage vector. A block diagram of the detection of input voltage angle is shown in Fig. 6. By using this simple method, a constant magnitude input voltage vector that rotates at a constant angular velocity can be made.

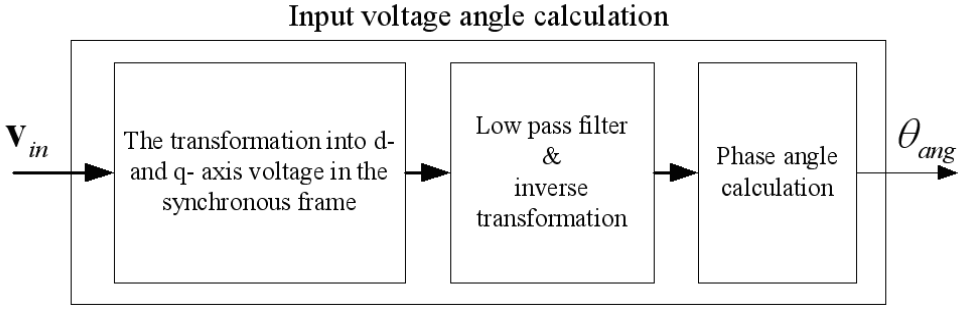

Figure 6: The block diagram of the displacement angle calculator.

It can be seen from Fig. 5 and Fig. 6 that the presented DTC scheme retains the advantages of the conventional DTC, such as very simple control structure without coordinate transformation and no current control loop, and keeps unity input power factor. However, in (15), the stator resistance is still a key parameter in influencing the proposed DTC performance. The stator resistance is estimated under operation by an adaptive observer [12].

4.3 Non-linearity compensation

The control structure shown in Fig. 1 uses the measured power grid voltages and the output current. The performance of the system is very sensitive to the knowledge of output voltage and therefore the matrix converter has to be modelled as in a voltage source inverter where the influence from the commutation delay and the voltage drop in the power devices exist [3].

4.3.1 Commutation delay

Switch commutation is an important issue when operating a matrix converter. When the current has to be commutated from one switch to another, it should be done in a four-step operation in order to avoid circulating currents [1]. This strategy keeps both transistors in the switch turned on while the switch is conducting. In this method there is no need to perform the inter-switch commutation by means of some logic circuit. As the current changes sign, the conducting diode will turn off naturally, and the load current will be taken over by the opposite conducting branch.

Fig. 7 shows two subsequent commutations for both current signs. The output voltage is shown with the control signals for the four transistors involved. In both cases the load current is positive and the input voltage, V_2, is greater than V_1. The conducting transistors are denoted by 1c and 2c whereas the non-conducting transistors are denoted by 1nc and 2nc.

In Commutation 1, before the commutation process is started, the output voltage equals V_2. When the commutation process is terminated, the output voltage will be equal to V_1. As $V_2 > V_1$, the series diode in the positive conducting transistor in switch 1 is reverse-biased, and no commutation takes place before the conducting transistor in switch 2 is turned off at a delay time T_d later. This results in a hard-switched commutation. In Commutation 2, the polarity of the commutation voltage is opposite. The diode in the conducting branch of the switch that is about to be turned on will be forward-biased in the second step of the commutation process and a natural commutation will take place.

When the phase current i_s is positive, the turn-on and turn-off time error T_{err} due to the commutation delay is calculated from Fig. 7 as

$$T_{err} = T_d + T_f - T_r \tag{16}$$

where T_r is the rise time of the switching device and T_f is the fall time of the switching device.

In a similar way, the turn-on and turn-off time error when phase current i_s is negative is calculated as

$$T_{err} = -(T_d + T_f - T_r). \tag{17}$$

From (16) and (17), these equations can be summarized as

$$T_{err} = (T_d + T_f - T_r) \cdot \mathrm{sgn}(i_s), \tag{18}$$

$$v_{cd} = \frac{T_{err}}{T_{sp}} v_{l-l} = v_{cd} \cdot \mathrm{sgn}(i_s), \tag{19}$$

where T_{sp} is the switching period, v_{l-l} is the line-to-line input voltage, and $v_{cd} = \frac{T_d + T_f - T_r}{T_{sp}} v_{l-l}$.

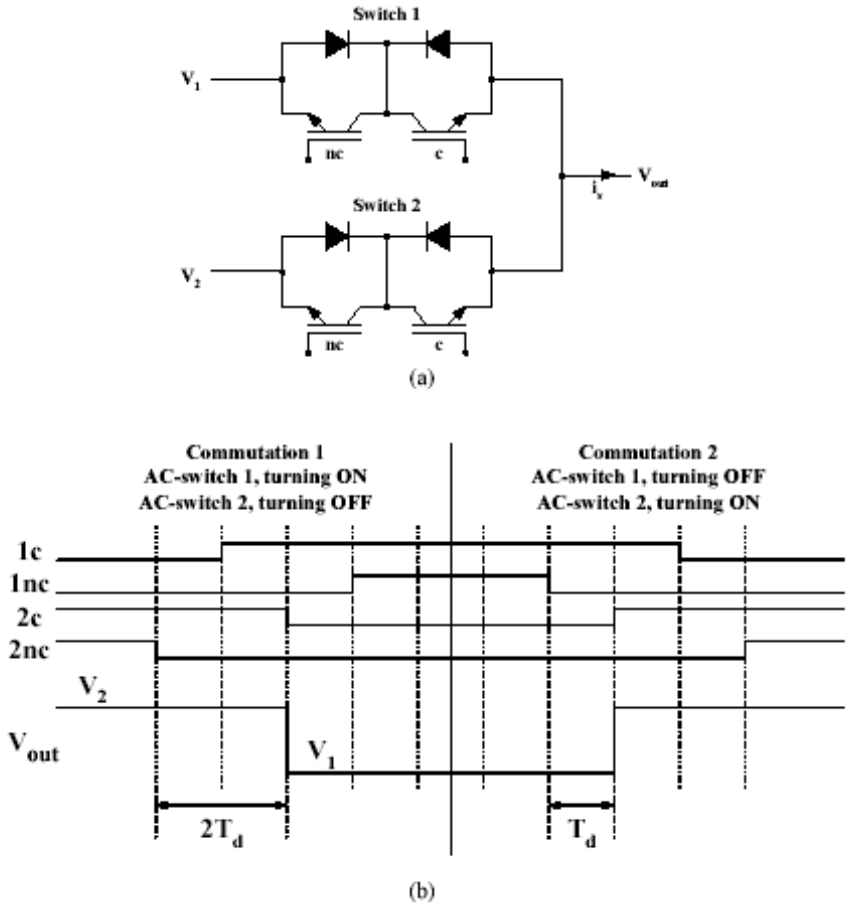

Figure 7: Four-step commutation strategy in a matrix converter. (a) Structure of the bi-directional switch topology, (b) Four-step commutation sequence (i_s>0).

The voltage error due to commutation delay in each phase can be transformed to a synchronous frame by employing the concept of field orienta-

tion as

$$\begin{aligned}
\begin{bmatrix} v^s_{q,\,cd} \\ v^s_{d,\,cd} \end{bmatrix} &= \tfrac{2}{3} \begin{bmatrix} \cos(0) & \cos\left(-\frac{2\pi}{3}\right) & \cos\left(\frac{2\pi}{3}\right) \\ \sin(0) & \sin\left(-\frac{2\pi}{3}\right) & \sin\left(\frac{2\pi}{3}\right) \end{bmatrix} \begin{bmatrix} v_{a,\,cd} \\ v_{b,\,cd} \\ v_{c,\,cd} \end{bmatrix} \\
&= v_{cd} \cdot \tfrac{2}{3} \begin{bmatrix} 1 & -\frac{1}{2} & -\frac{1}{2} \\ 0 & -\frac{\sqrt{3}}{2} & \frac{\sqrt{3}}{2} \end{bmatrix} \begin{bmatrix} \mathrm{sgn}\left(\mathrm{i_{as}}\right) \\ \mathrm{sgn}\left(\mathrm{i_{bs}}\right) \\ \mathrm{sgn}\left(\mathrm{i_{cs}}\right) \end{bmatrix} \\
= v_{cd} \cdot \begin{bmatrix} \frac{2}{3} & -\frac{1}{3} & -\frac{1}{3} \\ 0 & -\frac{\sqrt{3}}{3} & \frac{\sqrt{3}}{3} \end{bmatrix} &\begin{bmatrix} \mathrm{sgn}\left(\mathrm{i^e_{qs}} \cos\left(\hat{\theta}\right) + \mathrm{i^e_{ds}} \sin\left(\hat{\theta}\right)\right) \\ \mathrm{sgn}\left(\mathrm{i^e_{qs}} \cos\left(\hat{\theta} - \frac{2\pi}{3}\right) + \mathrm{i^e_{ds}} \sin\left(\hat{\theta} - \frac{2\pi}{3}\right)\right) \\ \mathrm{sgn}\left(\mathrm{i^e_{qs}} \cos\left(\hat{\theta} + \frac{2\pi}{3}\right) + \mathrm{i^e_{ds}} \sin\left(\hat{\theta} + \frac{2\pi}{3}\right)\right) \end{bmatrix}
\end{aligned} \tag{20}$$

where subscript 'e' denotes the variable in the synchronous reference frame and θ_r is the electrical rotor position.

4.3.2 Voltage drop in switching devices

Using the implementation shown in Fig. 1, the voltage drop in the matrix converter may be higher than that of the conventional inverter causing a severe disturbance at very low speeds, because two devices are always conducting. The threshold voltage of the power device has to be modeled to improve the performance at low-speed operation. If the forward voltage of the power devices can be approximated by a fixed-threshold value, v_{th}, the voltage drop across the power devices is generally characterized as

$$v_{drop} = R_d i_s + 2v_{th}. \tag{21}$$

The resistance R_d of the power device simplifies a linear relation between the load current and the inverter voltage as shown in Fig. 8 and therefore it can be added to the value of the stator resistance. The value of R_d is estimated using an adaptive estimation method [12].

The on-state voltage drop is dependent on the direction of the phase current. Fig. 9 shows the voltage drop influence on the output voltage. The voltage drop in each phase can be transformed to the synchronous reference frame as

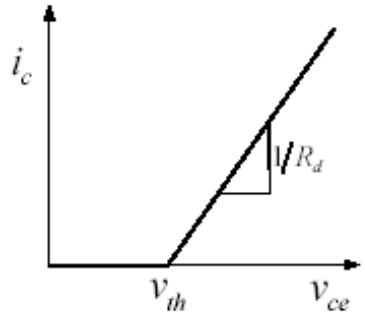

Figure 8: Simplified forward on-state characteristics of the power device.

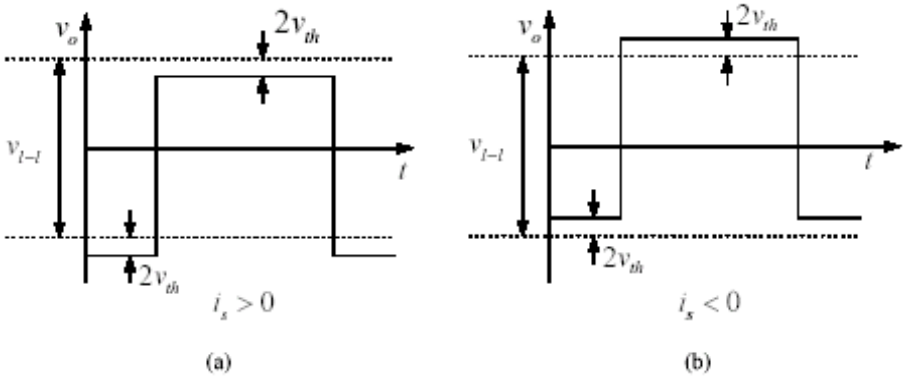

Figure 9: Output voltage in the matrix converter due to voltage drop across the power devices: (a) $i_s > 0$, (b) $i_s < 0$.

$$\begin{bmatrix} v^s_{q,drop} \\ v^s_{d,drop} \end{bmatrix} = v_{drop} \cdot \begin{bmatrix} \frac{2}{3} & -\frac{1}{3} & -\frac{1}{3} \\ 0 & -\frac{\sqrt{3}}{3} & \frac{\sqrt{3}}{3} \end{bmatrix} \cdot \begin{bmatrix} \operatorname{sgn}\left(\mathrm{i}^{\mathrm{e}}_{\mathrm{qs}} \cos\left(\hat{\theta}\right) + \mathrm{i}^{\mathrm{e}}_{\mathrm{ds}} \sin\left(\hat{\theta}\right)\right) \\ \operatorname{sgn}\left(\mathrm{i}^{\mathrm{e}}_{\mathrm{qs}} \cos\left(\hat{\theta} - \frac{2\pi}{3}\right) + \mathrm{i}^{\mathrm{e}}_{\mathrm{ds}} \sin\left(\hat{\theta} - \frac{2\pi}{3}\right)\right) \\ \operatorname{sgn}\left(\mathrm{i}^{\mathrm{e}}_{\mathrm{qs}} \cos\left(\hat{\theta} + \frac{2\pi}{3}\right) + \mathrm{i}^{\mathrm{e}}_{\mathrm{ds}} \sin\left(\hat{\theta} + \frac{2\pi}{3}\right)\right) \end{bmatrix}. \tag{22}$$

From (20) and (22), the total distortion voltage due to commutation delay and on-state switching device voltage drop are calculated as

$$\begin{bmatrix} v^s_{q,total} \\ v^s_{d,\,total} \end{bmatrix} = (v_{cd} + v_{drop}) \cdot \frac{2}{3} \begin{bmatrix} \frac{2}{3} & -\frac{1}{3} & -\frac{1}{3} \\ 0 & -\frac{\sqrt{3}}{3} & \frac{\sqrt{3}}{3} \end{bmatrix} \cdot \begin{bmatrix} \operatorname{sgn}\left(\mathrm{i}^{\mathrm{e}}_{\mathrm{qs}} \cos\left(\hat{\theta}\right) + \mathrm{i}^{\mathrm{e}}_{\mathrm{ds}} \sin\left(\hat{\theta}\right)\right) \\ \operatorname{sgn}\left(\mathrm{i}^{\mathrm{e}}_{\mathrm{qs}} \cos\left(\hat{\theta} - \frac{2\pi}{3}\right) + \mathrm{i}^{\mathrm{e}}_{\mathrm{ds}} \sin\left(\hat{\theta} - \frac{2\pi}{3}\right)\right) \\ \operatorname{sgn}\left(\mathrm{i}^{\mathrm{e}}_{\mathrm{qs}} \cos\left(\hat{\theta} + \frac{2\pi}{3}\right) + \mathrm{i}^{\mathrm{e}}_{\mathrm{ds}} \sin\left(\hat{\theta} + \frac{2\pi}{3}\right)\right) \end{bmatrix}. \tag{23}$$

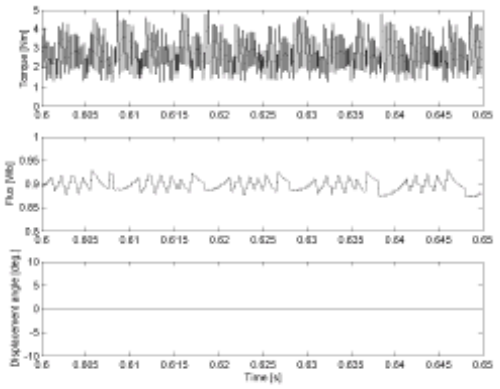

(a)

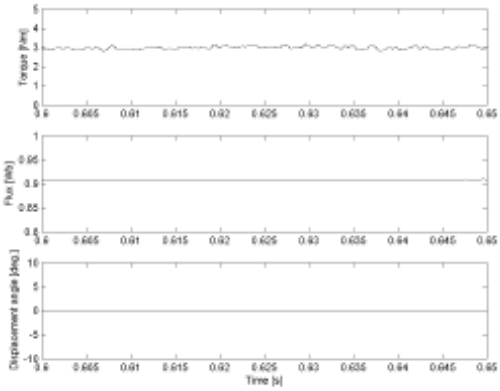

(b)

Figure 10: Torque, flux, input power factor control at 500 rpm with 50 % of rated load: (a) basic DTC, (b) proposed DTC-SVM (torque, flux, and displacement angle).

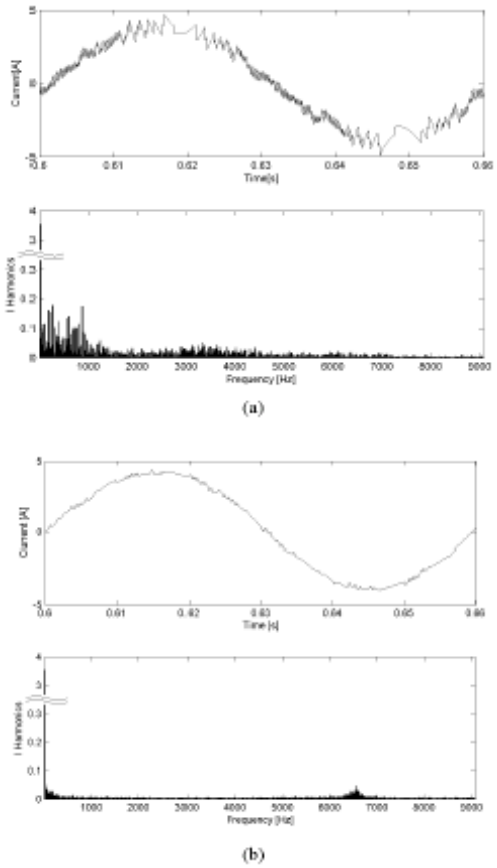

Figure 11: Phase current in time and frequency domains at 500 rpm with 50% of rated load: (a) basic DTC, (b) proposed DTC-SVM (phase current and harmonic spectrum).

The compensation for the non-linearity of the matrix converter drives is achieved by adding the distortion voltages.

5 Experiments

To confirm the validity of the proposed control algorithm, experiments were carried out. The system consists of a 3-phase, 380 V, 50 Hz, 4-pole, 3 kW induction motor and a power circuit with a matrix converter. A dual controller system consisting of a 32-bit DSP (ADSP 21062) and a 16-bit microcontroller (80C167), in conjunction with a 12-bit A/D converter board,

is used to control the matrix converter based induction motor drive. In the experiments, the sampling period is 90 μs for the hysteresis-band based DTC and 150 μs for the modified DTC using SVM and flux deadbeat control.

Figs. 10a and 10b show the experimental results of the steady state performance of the basic DTC and the proposed improved DTC at 500 rpm. The torque and flux ripple of the basic DTC are 2.5 Nm and 0.05 Wb, respectively. However, the torque and flux ripple of the proposed DTC is almost zero. It is seen from this result that the torque and flux ripple are reduced drastically by the proposed algorithm. The steady state phase current and its harmonic spectrums are compared in Figs. 11a and 11b. From Fig. 11a, a high distortion in the current can be observed and low order harmonics scattered from the fundamental to 4 kHz, which are not desirable.

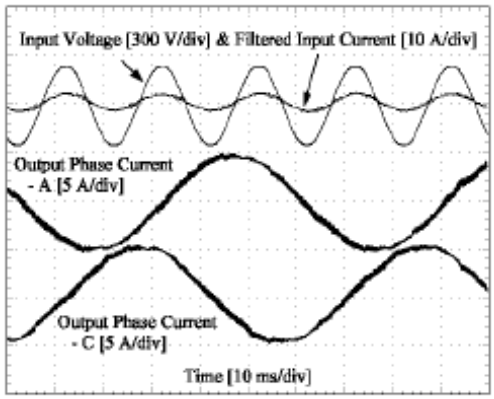

Figure 12: Filtered input current, input line-to-neutral voltage, output phase currents of the proposed improved DTC-SVM at 700 rpm with 20 % of rated load.

The current waveform of the proposed DTC in Fig. 11b is smoother than that of the basic DTC and the dominant harmonics are around 6.5 kHz which is determined by the SVM sampling period. Fig. 12 shows the filtered input line current and the corresponding line-to-neutral voltage. As it can be seen, the line current is in phase with the voltage, confirming the validity of the control scheme which allows unity input power factor operation. Fig. 13 shows the steady state characteristics of the speed and the phase current at 50 rpm. The nonlinearities cause undesired speed pulsations of about six times the electrical frequency, and the phase currrent is not pure sinusoidal

without nonlinearites compensation as shown in Fig. 13a. However, in the proposed DTC with a simple compensation scheme, the speed ripple and the distortion in the phase current waveform are remarkably reduced as shown in Fig. 13b.

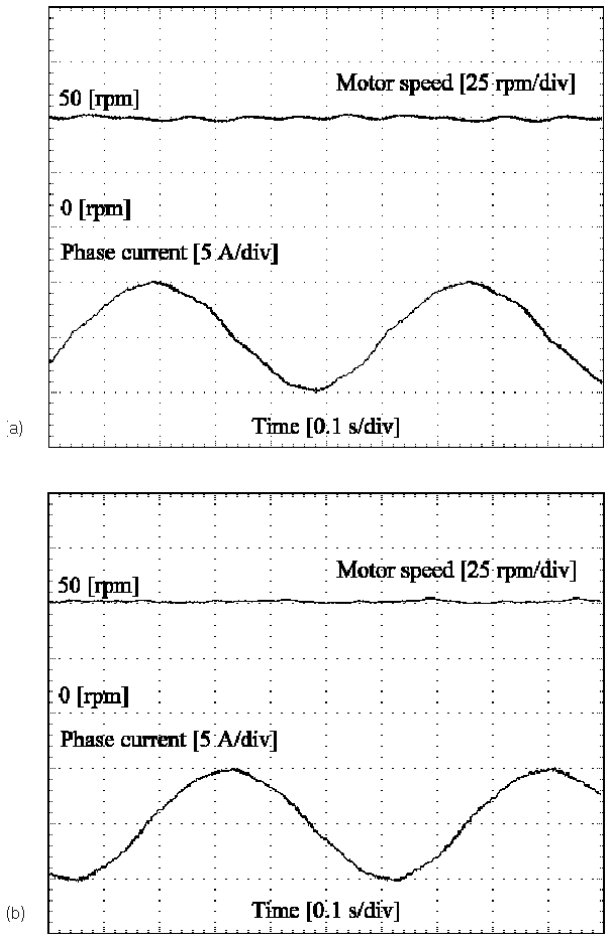

Figure 13: Experimental results of speed sensorless control at 50 rpm with 70 % of rated load; speed and phase current (a) without non-linearity compensation, (b) with non-linearity compensation.

6 Conclusion

In order to realize high performance control of induction motor drives fed by a matrix converter, a new DTC method for matrix converter drives has been proposed in this paper. The proposed method using SVM and deadbeat strategy enables to minimize torque ripple and to obtain unity input power factor while maintaining constant switching frequency. It can be said from the experimental results that torque, flux, input power factor, and sensorless speed control performance are improved with the proposed modified DTC.

References

[1] M.P. Kazmierkowski, R. Krishnan, and F. Blaabjerg, *Control in Power Electronics – Selected Problems*, Ch. 3 (Academic Press, 2002).

[2] P.W. Wheeler, J. Rodriguez, J.C. Clare, L. Empringham, and A. Weinstein, IEEE Trans. on Industrial Electronics **49**, 279 (2002).

[3] K.B. Lee and F. Blaabjerg, Proc. PESC'04, p.1341 (2004).

[4] D. Casadei, G. Serra, and A. Tani, IEEE Trans. on Industrial Electronics **48**, 1057 (2001).

[5] K.B. Lee, J.H. Song, I. Choy, and J.Y. Yoo, IEEE Trans. on Power Electronics **17**, 255 (2002).

[6] M. Fu and L. Xu, Proc. IEEE PESC'99, p.159 (1999).

[7] D. Swierczynski, M.K. Kazmierkowski, and F. Blaabjerg, Proc. IEEE ISIE'02, p.723 (2002).

[8] L. Tang, L. Zhong, M.F. Rahman, and Y. Hu, IEEE Trans. on Power Electronics **19**, 346 (2004).

[9] C. Lascu, I. Boldea, and F. Blaabjerg, IEEE Trans. on Industrial Electronics **51**, 785 (2004).

[10] B.H. Kenny and R.D. Lorenz, IEEE Trans. on Industry Applications **39**, 1093 (2003).

[11] T.G. Habetler, F. Profumo, M. Pastorelli, and L.M. Tolbert, IEEE Trans. on Industry Applications **28**, 1045 (1992).

[12] K.B. Lee, J.H. Song, I. Choy, and J.Y. Yoo, IEEE Trans. on Industrial Electronics **48**, 1006 (2001).